J. Phys. Earth, **29**, 537–557, 1981

A STATISTICAL MODEL FOR PREDICTION OF QUASI-REALISTIC STRONG GROUND MOTION

Yasuo IZUTANI

Department of Civil Engineering, Faculty of Engineering, Shinshu University, Nagano, Japan

(Received June 10, 1981; Revised November 6, 1981)

The total power, the duration, and the starting time of band-pass filtered accelerograms are chosen as model parameters to express amplitude variations of ground acceleration in both the time and frequency domains. In order to estimate model parameters of certain earthquakes and site conditions, a probabilistic source model is used and accelerograms recorded during the Matsushiro earthquake swarm are analyzed statistically. The duration and the starting time of the strong ground motion are found to have close relations to the amplification characteristics of surface layers at the sites. As an example, model parameters are estimated by assuming the source parameters and the site conditions of the Miyagi-Oki earthquake of June 12, 1978. Wave-forms, running spectra, and velocity response spectra of synthetic accelerograms resemble those of observed accelerograms.

1. *Introduction*

Not only recorded accelerograms (e.g., El Centro, 1940; Taft, 1952) but also realistic accelerograms of future earthquakes are needed for the data of actual earthquake resistant design. The purpose of this study is to develop quasi-realistic synthetic accelerograms by combining statistical estimates of source and path effects with site properties from HASKELL's (1960) method.

A source model, such as HASKELL's (1964), can satisfactorily account for observed long-period seismic waves but not short-period seismic waves. Therefore, an approach basing on a source model has seldom been used for the purpose of earthquake engineering, and so statistical models for predicting strong earthquake ground motion usually disregard the source model (e.g., GOTO *et al.*, 1979; KATADA and HOSHIYA, 1980). However, since such statistical models are derived from a multiple regression analysis, their application is limited to the range of the data set which was analyzed. Moreover, since the magnitude and the epicentral distance are normally used as the predictor variables in the regression equations, such statistical models are not suitable to express the empirical fact concerning the amplitude of near-field strong ground motion (i.e., "The seismic motion near a fault depends neither on fault length nor on fault width once they exceed certain limits, but is determined mostly by the dislocation time-function and velocity of rupture propagation."—AKI, 1972).

HIRASAWA (1980) presented a probabilistic source model in order to explain the amplitude of short-period seismic waves. Since the stress-drop on a fault is treated probabilistically, the main parameter in the model is the root-mean-square (rms) of the stress-drop. Generally, the rms stress-drop is larger than the mean stress-drop, so that the amplitude of short-period seismic waves predicted by this source model is larger than that expected from the deterministic source models. In this study, Hirasawa's source model is used to estimate the amplitude of near-field strong ground motion to avoid difficulties inherent in statistical prediction models.

Site conditions are closely correlated to the disaster due to earthquake. For example, SEED *et al.* (1972) reported that there was a strong correlation between the number of floors of damaged buildings and the thickness of sediments, in the Caracas earthquake of 1967. Therefore the actual frequency response characteristics of the ground must be used in synthesizing strong ground motion, rather than the conventional classification, "type of ground." Also, the duration of strong motion is strongly influenced by the site conditions (e.g., TRIFUNAC and BRADY, 1975; DOBRY *et al.*, 1978). Since both the amplitude and the duration play important roles in the elastic-plastic response of structures or in the liquefaction of sandy ground, one of the purposes of this study is to consider the influence of site condition on the duration.

2. *Data Analyzed*

We will analyze 44 horizontal component accelerograms recorded during the Matsushiro earthquake swarm from 1965 to 1970 (OSAWA *et al.*, 1976).

Table 1. Data set.*

Earthquake	Magnitude	Depth (km)	Observation station** (Distance, km)
M- 53	5.1	4.3	1 (4.0), 3 (3.0)
M- 74	4.7	5.6	1 (3.5)
M- 95	4.5	3.6	1 (5.5)
M-123	4.9	5.5	1 (2.5), 4 (4.0)
M-147	4.7	3.2	4 (1.5)
M-169	4.6	6.8	2 (6.5), 3 (10.5), 4 (7.5)
M-186	4.2	5.0	2 (3.0)
M-192	4.6	4.8	3 (4.5)
M-219	4.4	4.8	2 (2.0), 3 (4.5), 4 (5.5)
M-262	5.0	3.2	4 (6.5)
M-270	4.7	5.5	2 (2.0), 3 (4.0), 4 (5.0)
M-322	5.0	7.0	4 (9.0)
M-329	4.4	3.2	2 (4.5)
M-425	4.5	2.0	2 (2.5)

* OSAWA *et al.* (1976). ** 1, Hoshina-A; 2, Hoshina-B; 3, Wakaho; 4, Matsushiro-C.

The maximum acceleration of each accelerogram ranges from 71 to 392 gal. As shown in Table 1, the JMA magnitudes of these earthquakes range from 4.2 to 5.1, and the epicentral distance ranges from 1.5 to 10.5 km. Although a data set which contains accelerograms over a wide distance range is generally preferable, this data set is well-suited for a detailed study of the influence of site condition on the amplitude and the duration of strong ground acceleration, because it contains many near-field accelerograms recorded at only four sites.

3. *Model Parameters*

In order to treat accelerograms statistically, it is necessary to express the characteristics of the ground acceleration in both the time and frequency domains in terms of certain model parameters. Although various definitions of strong-motion parameters were presented (e.g., BOLT, 1973; TRIFUNAC and BRADY, 1975; MCCANN and SHAH, 1979), we use the following definition, which is similar to that of TRIFUNAC and BRADY (1975).

The ground acceleration, $x(t)$, is filtered by a narrow band-pass filter, $h_i(t)$, then the total power, E_i, and the cumulative power curve, $P_i(t)$, of filtered acceleration are calculated as

$$\left.\begin{aligned} y_i(t) &= x(t) * h_i(t)\,, \\ E_i &= \int_0^{T_d} [y_i(t)]^2 \, dt\,, \\ P_i(t) &= \frac{1}{E_i} \int_0^t [y_i(t)]^2 dt\,, \end{aligned}\right\} \tag{1}$$

where T_d is the total duration of the filtered accelerogram. In Fig. 1, an example of the cumulative power curve, $P_i(t)$, is shown by a solid line. The starting time, t_i, and the duration, D_i, of the filtered strong motion are defined as the time at $P_i(t)=0.05$ and the time required for $P_i(t)$ to increase from 0.05 to 0.85,

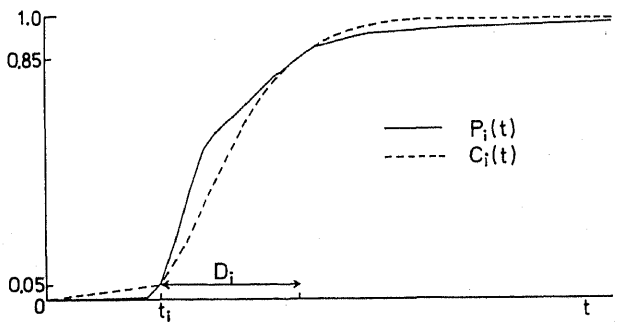

Fig. 1. An example of cumulative power curve, $P_i(t)$, of filtered accelerogram and its approximation function, $C_i(t)$. D_i and t_i indicate the duration and the starting time of the strong ground motion.

respectively. Then, $P_i(t)$ is approximated by a function, $C_i(t)$, that is expressed by the two parameters, t_i and D_i, as

$$C_i(t)=\begin{cases}(0.05/t_i)t; & 0\leqq t<t_i\,,\\ 1-\{2a^2(t-b)^2+2a(t-b)+1\}e^{-2a(t-b)}; & t_i\leqq t\,,\end{cases}\qquad \begin{cases}a=1.955/D_i\,,\\ b=t_i-0.210/D_i\,.\end{cases} \tag{2}$$

$C_i(t)$ is shown by a broken line in Fig. 1. Therefore, the variation of amplitude of the filtered acceleration with time can be expressed by the three parameters, E_i, D_i and t_i.

The filter, $h_i(t)$, is assumed to have the velocity response of a one degree of freedom oscillator,

$$h_i(t)=4\pi h f_i\{\cos\omega_d t-h_d\sin\omega_d t\}e^{-2\pi h f_i t}\,,\qquad \begin{cases}\omega_d=2\pi f_i\sqrt{1-h^2}\,,\\ h_d=h/\sqrt{1-h^2}\,,\end{cases} \tag{3}$$

where f_i and h are the natural frequency and the damping coefficient of the oscillator, respectively. If the damping coefficient is small, the filter is sharp and the spectral shape of acceleration is well expressed but the change of acceleration with time becomes unclear. h may be reasonably assumed to be 0.1.

Considering the accuracy and the computational time of the synthesized accelerogram (how it is made is described in Appendix), the number of filters is chosen to be 12. The central frequencies of the filters are chosen to be equally spaced on the logarithmic scale from $\log f_1=-0.64$ to $\log f_{12}=1.12$.

Generally, the model parameters obtained from the two horizontal component accelerograms at the same station for the same earthquake differ from each other. This is especially true for E_i, for which the difference sometimes amounts to a factor of 3 or 4. This seems to be caused mainly by the radiation pattern of seismic waves. However, since no account of radiation pattern is taken of in this study, the definitions of model parameters should be changed (except in Appendix) as follows; E_i is the sum of total power of the two horizontal component filtered accelerations. D_i is the average of the two durations weighted by total power. t_i is the average of the two starting times.

4. *Estimation of E_i*

4.1 Source spectrum

We now suppose a source spectrum of acceleration as illustrated by a solid line in Fig. 2. At frequencies much higher than f_c, the so-called "corner frequency," the spectral density is given by HIRASAWA's (1980) model. The amplitude ratio of the spectrum by HIRASAWA's (1980) model to that by the deterministic source model is assumed to be $\sqrt{\mathrm{E}\{\tau^2\}}/\mathrm{E}\{\tau\}$. The corner frequency is estimated by means of the experimental relation of FURUYA (1969),

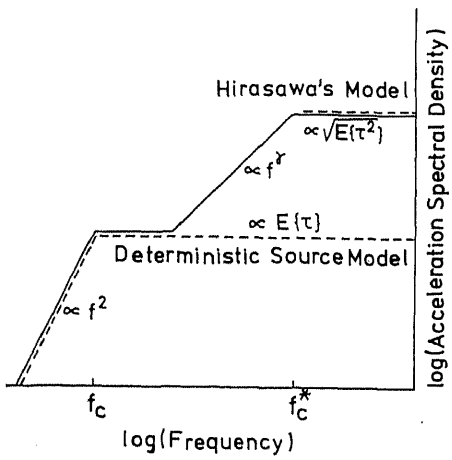

Fig. 2

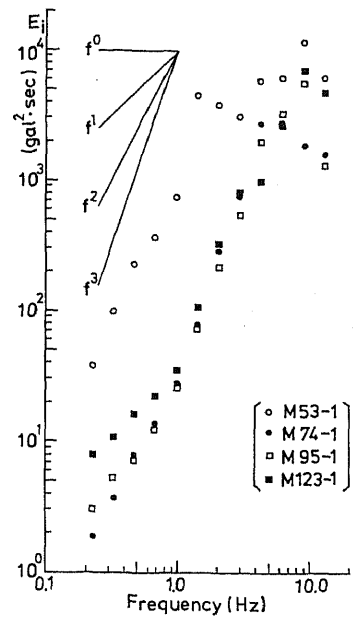

Fig. 3

Fig. 2. Supposed source spectrum. The solid line indicates the source spectrum supposed in this study. Dashed lines are those expected from HIRASAWA's (1980) model and the deterministic source model. f_c is the so-called "corner frequency" and f_c^* is the characteristic frequency of the supposed spectrum.

Fig. 3. Total power, E_t, of the filtered accelerograms at Hoshina-A.

$$\log f_c = 1.2 - 0.4M \,. \tag{4}$$

Using the relation between the magnitude, M, and the fault diameter, L, by OTSUKA (1964),

$$\log L = 0.5M - 1.8 \,, \tag{5}$$

(4) is transformed as

$$\log f_c = -0.24 - 0.8 \log L \,. \tag{6}$$

The spectral density below f_c is considered to be proportional to f^2 according to the deterministic source models. However, since the frequency, f_c^*, is not given by HIRASAWA's (1980) model, it will be estimated by analyzing the recorded accelerograms in Sec. 4.3.

The trend of the spectral density curve below f_c^* is also unknown. In Fig. 3, the total powers, E_t, of the filtered accelerograms for four earthquakes observed at Hoshina-A are shown. According to the spectral shape of microtremors by KANAI *et al.* (1966), Hoshina-A seems to be a rock site, so the influence of the surface layers on E_t is negligible. Also, the attenuation effect due to anelastic-

ity of the medium is not removed because of the small epicentral distances. The corner frequencies estimated by (4) are around 0.2 Hz. Comparing Fig. 3 with Fig. 2, it seems that f_c* is around 1 Hz for M53-1 and around 5 Hz for the other accelerograms. E_i between 0.2 and 1.5 Hz for M53-1 and between 1 and 5 Hz for the others seem to be proportional to f^3. Since the effect of the band-pass filter of E_i is proportional to f^1, γ in Fig. 2 is equal to 1.

4.2 Expression for estimating E_i

According to HIRASAWA (1980), the acceleration due to S waves radiated from a circular fault with radius R can be approximated by a random pulse sequence. The length of the pulse sequence is about R/v_R, where v_R is the rupture velocity. If the pulses are observed at a distance r from the fault, they can be considered to be radiated from the center of the fault, with power spectral density

$$S(\omega)=0.076\frac{v_S^3}{R}\frac{\mathrm{E}\{\tau^2\}}{\mu^2}F(\alpha r, R/r)\,, \tag{7}$$

where v_S is the S-wave velocity, μ is the rigidity, and the rupture velocity is assumed to be 75% of v_S. τ is the stress-drop at a small fault element and $\mathrm{E}\{\tau^2\}$ is the mean-square value of τ on the fault. $F(\alpha r, R/r)$ is the term caused by the difference of attenuation due to the difference of distances between each of the fault elements and the observation station. α is defined as

$$\alpha\equiv\pi f/v_S Q\,, \tag{8}$$

where f is the frequency and Q is the quality factor of the medium.

According to OTSUKA (1979), the solid angle, Ω, in regard to a fault at a station has a strong relation to the maximum acceleration and the intensity of ground shaking. Since the solid angle can be approximated by the function $F(\alpha r, R/r)$

$$\Omega\equiv 2\pi\left\{1-\frac{1}{\sqrt{1+(R/r)^2}}\right\}\approx\pi F(0.4, R/r)\,, \tag{9}$$

$F(\alpha r, R/r)$ in (7) is replaced by Ω/π for simplicity.

In order to obtain the total power, $\tilde{E}_i$, of the filtered ground acceleration, the attenuation, $\exp(-\alpha r)$, due to Q of the medium, the ground response, $|G(\omega)|$, and the response, $|H_i(\omega)|$, of the band-pass filter must be taken into account. Assuming that $\exp(-\alpha r)$ and $|G(\omega)|$ are smooth enough in comparison with the band width of the filter, they are approximated with the values at the central frequency of the filter. Therefore,

$$\tilde{E}_i\approx\frac{0.1}{\pi}\cdot\frac{v_S^2}{\mu^2}\cdot\mathrm{E}\{\tau^2\}\cdot\Omega\cdot\exp(2\pi f_i r/v_S Q)\cdot c_T^2\cdot|G(f_i)|^2\cdot\int_{-\infty}^{\infty}|H_i(\omega)|^2\mathrm{d}\omega\,, \tag{10}$$

where the relation $v_R=0.75v_S$ is assumed, and c_T is the transmission coefficient of the wave from the medium at the source region to the basement rock under the site.

Moreover, using an approximation,

$$\log\left\{\int_{-\infty}^{\infty}|H_i(\omega)|^2\mathrm{d}\omega\right\}\approx 0.60+\log f_i\,, \tag{11}$$

the total power of the filtered acceleration is obtained as

$$\begin{aligned}\log\tilde{E}_i=&c+2\log\sqrt{\mathrm{E}\{\tau^2\}}+\log\Omega+\log f_i\\&-2.73f_ir/v_\mathrm{S}Q+2\log|G(f_i)|\,,\\c=&1.11-2\log v_\mathrm{S}-2\log\rho+2\log c_\mathrm{T}\,,\end{aligned} \tag{12}$$

where the constant, c, contains the correction coefficient to express the parameters in the following units; $\tilde{E}_i$ in gal^2·sec, $\sqrt{\mathrm{E}\{\tau^2\}}$ in bar, ρ in g/cm^3 and v_S in km/sec. For simplicity, $|G(f_i)|$ may be assumed to be the response of surface layers to the vertical incidence of plane SH waves.

Since HIRASAWA (1980) neglected the effect of the radiation pattern, $\tilde{E}_i$ in (12) probably overestimates the total power of the single horizontal component of filtered acceleration. We roughly assume that $\tilde{E}_i$ in (12) gives the estimated value of E_i, the sum of total power of the two horizontal component filtered accelerations. Considering the source spectrum described in the preceding section, the expressions for estimating E_i are given as

$$\log E_i=\begin{cases}c+2\log\sqrt{\mathrm{E}\{\tau^2\}}+\log\Omega+\log f_i\\\quad -2.73f_ir/v_\mathrm{S}Q+2\log|G(f_i)|; & f_\mathrm{c}{}^*\leqq f_i\,,\\c+2\log\sqrt{\mathrm{E}\{\tau^2\}}+\log\Omega+3\log f_i-2\log f_\mathrm{c}{}^*\\\quad -2.73f_ir/v_\mathrm{S}Q+2\log|G(f_i)|; & f_\mathrm{B}\leqq f_i<f_\mathrm{c}{}^*\,,\\c+2\log\mathrm{E}\{\tau\}+\log\Omega+\log f_i\\\quad -2.73f_ir/v_\mathrm{S}Q+2\log|G(f_i)|; & f_\mathrm{c}\leqq f_i<f_\mathrm{B}\,,\\c+2\log\mathrm{E}\{\tau\}+\log\Omega+5\log f_i-4\log f_\mathrm{c}\\\quad -2.73f_ir/v_\mathrm{S}Q+2\log|G(f_i)|; & f_i<f_\mathrm{c}\,,\end{cases} \tag{13}$$

where

$$f_\mathrm{B}=(\mathrm{E}\{\tau\}/\sqrt{\mathrm{E}\{\tau^2\}})f_\mathrm{c}{}^*\,. \tag{14}$$

4.3 Analysis of accelerograms for estimating $f_\mathrm{c}{}^*$

As shown in Table 1, parameters known for Matsushiro earthquakes are the magnitude, the epicentral distance, Δ, and the focal depth, d. The fault diameter, L, is estimated by the relation (5), and the hypocentral distance, r, is approximated as

$$r=(\Delta^2+d^2)^{1/2}\,. \tag{15}$$

KANAI *et al.* (1966) observed microtremors and determined the "type of ground" at the sites, but the ground response or the layer parameters are unknown. In order to estimate the ground response, $|G(f_i)|$, at each site, a multiple regression analysis is carried out using the equation,

$$\log E_i = b_0 + b_1 \log \Omega + b_2 r + \sum_{j=1}^{3} g_{ij} x_j \,, \tag{16}$$

where x_j are dummy variables about the sites and take the values (0, 0, 0) for Hoshina-A, (1, 0, 0) for Hoshina-B, (0, 1, 0) for Wakaho, and (0, 0, 1) for Matsushiro-C. Then, the partial regression coefficients, g_{ij}, approximately give the ground response at each site. Using the assumption, $|G(f_i)|=2.0$ at Hoshina-A because of the rock site,

$$|G^{(j)}(f_i)| \approx 2.0 \times 10^{g_{ij}/2} \,. \tag{17}$$

Now, the best fit values of $\mathrm{E}\{\tau\}$, $\sqrt{\mathrm{E}\{\tau^2\}}$ and f_c* are determined by minimizing the sum of the squares of the residuals between the observed $\log E_i$ and those calculated by (13). The results are shown in Table 2. As the accelerograms contain not only the S waves but also the P wave and the surface waves while the values of $\mathrm{E}\{\tau\}$ and $\sqrt{\mathrm{E}\{\tau^2\}}$ in Table 2 are obtained from the expressions in (13), these values may not exactly indicate the mean and the rms of the stress-drop. However, it seems reasonable that these values approximate the mean and rms of the stress-drop. As shown in Fig. 4, $\log f_c$* has a linear correlation with $\log(\sqrt{\mathrm{E}\{\tau^2\}}/\mathrm{E}\{\tau\})$, and by means of the least squares method,

Table 2. Best fit parameters of source spectrum.

Earthquake-station	$\mathrm{E}\{\tau\}$ (bar)	$\sqrt{\mathrm{E}\{\tau^2\}}$ (bar)	f_c* (Hz)
M 53-1	27	63	1.3
M 74-1	9.2	55	3.6
M 95-1	14	75	4.4
M123-1	12	54	5.0
M169-2	13	119	5.8
M186-2	11	89	7.3
M219-2	11	48	2.9
M270-2	13	61	2.4
M329-2	18	74	2.5
M425-2	7.6	32	3.6
M 53-3	15	51	2.8
M169-3	14	186	8.7
M192-3	21	87	3.5
M219-3	13	85	4.9
M270-3	10	32	1.8
M123-4	9.8	54	2.9
M147-4	18	53	2.3
M169-4	12	84	4.1
M219-4	12	95	4.8
M262-4	21	59	3.1
M270-4	11	48	2.7
M322-4	32	90	4.4

$\mathrm{E}\{\tau\}$, average value of stress-drop; $\sqrt{\mathrm{E}\{\tau^2\}}$, root-mean-square of stress-drop; f_c*; characteristic frequency.

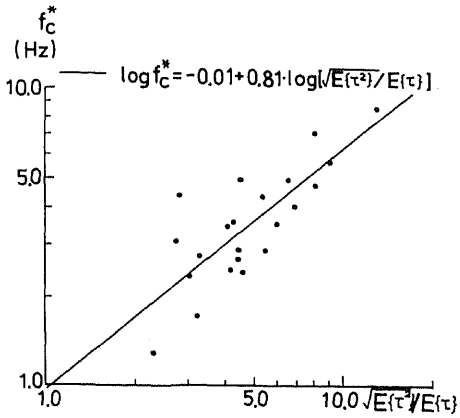

Fig. 4. The relation between the characteristic frequency, f_c^*, and the ratio of rms stress-drop to average stress-drop. The solid line indicates the best fit linear function by the least squares method.

$$\log f_c^* = -0.01 + 0.81 \log(\sqrt{E\{\tau^2\}}/E\{\tau\}) \pm 0.116 , \tag{18}$$

is obtained.

5. *Estimation of D_i*

5.1 *Expression for estimating D_i*

The duration, D_i, of the filtered acceleration is defined as the time required for the cumulative power curve to increase from 0.05 to 0.85. We will obtain the expression for estimating D_i by analyzing the observed accelerograms statistically.

The duration of strong ground motion is influenced by the condition of source, propagating path and surface layers at a site. It may be natural to think that the duration becomes longer with increasing hypocentral distance. According to the results of multiple regression analysis about duration by TRIFUNAC and BRADY (1975) and by DOBRY *et al.* (1978), however, it seems very difficult to express exactly the influence of path length on the duration. Considering that the source has finite dimensions and that the fracture of the fault propagates with a finite velocity, the difficulty increases especially in treating the duration of near-field ground motion. Moreover, since the model parameter, D_i, indicates the duration of the band-pass filtered acceleration, the effect of dispersion is not very significant. In the following, the influence of the hypocentral distance on D_i will not be considered.

As shown in Fig. 5, the average values of D_i at Hoshina-A are approximated as

$$\bar{D}_i = 0.15\bar{L} + 1.0/f_i , \tag{19}$$

where $\bar{L}$ is the average value of L. Since the accelerograph is assumed to rest on

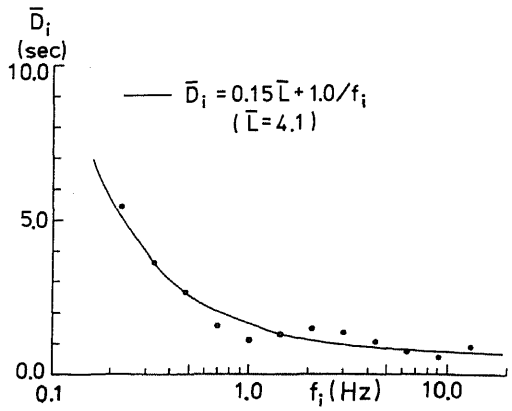

Fig. 5. Average value of duration of the filtered accelerograms at Hoshina-A. The solid line indicates the approximation function. $\bar{L}$ is the average value of the fault diameters of the earthquakes observed at Hoshina-A.

basement rock at this site, the influence of the site condition on D_i is negligible. The term, $1.0/f_i$, express the effect of the band-pass filter. Therefore, the influence of site condition on D_i at the other sites is estimated as

$$F_i = D_i - 0.15L - 1.0/f_i \,. \tag{20}$$

The cause of the influence of site condition is considered to be the multiple-reflection of seismic waves in the surface layers, and the influence on D_i may be related to the influence on E_i. As the first approximation, a relation,

$$[F_i^{(j)} - F_i^{(k)}] \propto [|G^{(j)}(f_i)| - |G^{(k)}(f_i)|] \,, \tag{21}$$

is assumed. Where, (j) and (k) indicate the sites. If the (k) station is assumed to be Hoshina-A, $F_i^{(k)}=0.0$, $|G^{(k)}(f_i)|=2.0$, and (21) becomes

$$F_i \propto [|G(f_i)|/2 - 1] \,. \tag{22}$$

The attenuation of seismic waves due to anelasticity in the surface layers seems to have a great influence on E_i but a little influence on D_i, because the direct wave is also attenuated as well as multiple-reflected waves. Then, rejecting the average effect of attenuation, e^{-kf}, from $|G(f_i)|$ as

$$|G^*(f_i)| = |G(f_i)|/e^{-kf_i} \,, \tag{23}$$

$|G(f_i)|$ in (22) is replaced by $|G^*(f_i)|$. The relation between $\bar{F}_i$, the average values of F_i at each site, and $|G^*(f_i)|$ is shown in Fig. 6, and it is approximated by a linear relation,

$$\bar{F}_i = 0.62\{|G^*(f_i)|/2 - 1\} \pm 0.84 \,. \tag{24}$$

In this case, referring to the spectral shape of microtremors observed by KANAI *et al.* (1966), the attenuation coefficient, k, due to anelasticity in the sur-

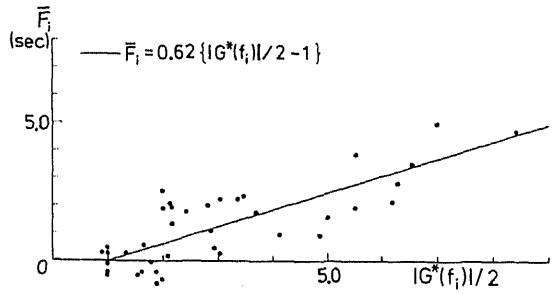

Fig. 6. The relation between the average effect, $\bar{F}_i$, of the site condition on the duration and the amplification characteristics of the surface layers. The solid line indicates the best fit linear function by the least squares method.

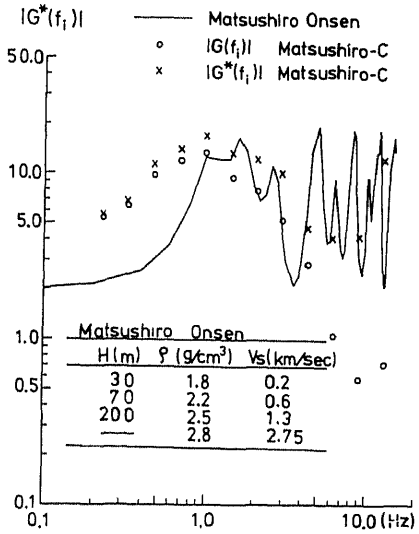

Fig. 7. Amplification characteristics of the surface layers at Matsushiro-C and Matsushiro-Onsen. $|G(f_i)|$ denotes the amplification by considering the effect of attenuation in the surface layers. $|G^*(f_i)|$ denotes the amplification by not considering the attenuation effect. The solid line indicates the amplification characteristics by using the layer parameters in this figure.

face layers is assumed to be 0.05 at Hoshina-B, 0.20 at Wakaho, and 0.23 at Matsushiro-C. $|G(f_i)|$ and $|G^*(f_i)|$ at Matsushiro-C are shown in Fig. 7. Layer parameters and the ground response calculated by HASKELL's (1960) method at Matsushiro-Onsen near Matsushiro-C are also shown in Fig. 7. The thicknesses of the layers are estimated from the result of drilling by the National Research Center for Disaster Prevention, while reasonable values of the S-wave velocities and the densities are assumed. Since $|G^*(f_i)|$ at Matsushiro-C well agrees with the amplitude level of the ground response at Matsushiro-Onsen in the high frequency range, the assumed value of k seems to be appropriate.

Therefore, the expression for estimating D_i is

$$D_i=0.15L+1.0/f_i+0.62\{|G^*(f_i)|/2-1\}\pm 0.84\,. \tag{25}$$

5.2 On the effect of fault diameter on D_i

The expression (25) for estimating D_i contains the parameter, L, the diameter, of the fault. Since the analyzed data set contains earthquakes whose fault diameters are limited within a narrow range, some errors may occur in the estimated values of D_i.

DOBRY *et al.* (1978) analyzed accelerograms on rock sites about the earthquakes whose magnitudes range from 4.5 to 7.6, and obtained a relation,

$$\log D^*=0.43M-1.83\,. \tag{26}$$

Substituting the relation (5) into (26),

$$\log D^*=0.86\log L-0.28 \tag{27}$$

is obtained. The definition of D^* is the time required for the cumulative power curve of the ground acceleration to increase from 0.05 to 0.95. About D_i^* at Hoshina-A

$$\bar{D}_i^*=0.31\bar{L}+1.5/f_i \tag{28}$$

is obtained by an analysis similar to what has been carried out about D_i. Since the high frequency components are predominant at Hoshina-A and the term, $1.5/f_i$, is mainly the result of influence of the band-pass filter, this term is neglected and the relation between D^* and L,

$$\log D^*=\log L-0.51 \tag{29}$$

is obtained. The two kinds of relation between D^* and L are shown in Fig. 8. Their discrepancy is not so significant. Therefore, the result of DOBRY *et al.* (1978) supports the relation between D_i and L in (25) indirectly.

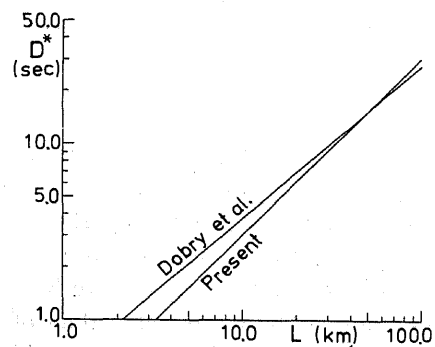

Fig. 8. Relations between the duration of strong ground motion, D^*, and the fault diameter, L. One of the relations was presented by DOBRY *et al.* (1978) and the other is obtained in the present study.

6. *Estimation of t_i*

The predominant energy of an accelerogram observed at near-field is contributed by S waves, so that the starting time of strong ground motion on the filtered accelerogram is about the onset time of S phase. It is expected that the time at $P_i(t)=0.05$, that is t_i, becomes more delayed with increasing the amplification effect of the surface layers. As shown in Fig. 9, the average values of t_i-t_{12} at each site have a linear relation to the ground response, $|G(f_i)|-|G(f_{12})|$. The relation is approximated as

$$\overline{t_i-t_{12}}=0.072\{|G(f_i)|-|G(f_{12})|\}\pm 0.084\,. \tag{30}$$

Assuming that t_{12} is equal to S—P time, t_i is estimated by

$$t_i=r\left(\frac{1}{v_S}-\frac{1}{v_P}\right)+0.072\{|G(f_i)|-|G(f_{12})|\}\pm 0.084\,. \tag{31}$$

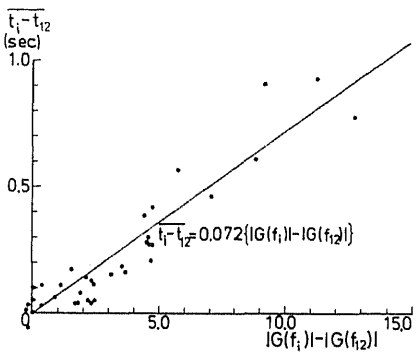

Fig. 9. The relation between the average values of starting time of the strong ground motion and the amplification characteristics of the surface layers. The solid line indicates the best fit linear function by the least squares method.

7. *Synthetic Accelerogram*

7.1 *Flow chart for obtaining synthetic accelerogram*

The procedure to calculate synthetic accelerograms is shown in Fig. 10. When the source parameters, L, $\mathrm{E}\{\tau\}$ and $\sqrt{\mathrm{E}\{\tau^2\}}$, the hypocentral distance, r, and the layer parameters at a site are given, the model parameters, E_i, D_i, and t_i, can be estimated. Then, using the simulation method presented in Appendix, sample accelerograms are synthesized. In Fig. 10, the numbers in parentheses denote the equation numbers in this paper. σ_{E_i} means the rms residuals between the observed values of $\log E_i$ and those calculated by (13), and $\sigma_{E_i}=0.16$ is obtained. σ_{D_i} is the standard deviation of F_i around $\bar{F}_i$ at each site, and $\sigma_{D_i}=0.88$ is obtained. σ_{t_i} is the standard deviation of t_i-t_{12} around $\overline{t_i-t_{12}}$ at each site, and it is related to $|G(f_i)|-|G(f_{12})|$ by

$$\sigma_{t_i}=0.04+0.05\{|G(f_i)|-|G(f_{12})|\}\pm 0.09\,. \tag{32}$$

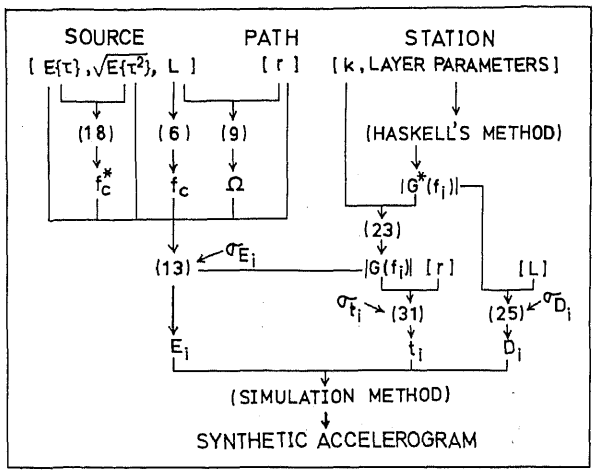

Fig. 10. Flow chart for obtaining synthetic accelerograms. The numbers in parentheses denote the equation numbers in this paper. $E\{\tau\}$, average stress-drop; $\sqrt{E\{\tau^2\}}$; rms of stress-drop; L, fault diameter; r, hypocentral distance; k, attenuation coefficient in surface layers; f_c*, characteristic frequency; f_c, corner frequency; Ω, solid angle of a fault; $|G^*(f_i)|$, amplification characteristics of surface layers by considering no attenuation; $|G(f_i)|$, amplification characteristics of surface layers; E_i, total power of filtered acceleration; D_i, duration of filtered acceleration; t_i, starting time of strong motion of filtered acceleration; σ_{E_i}, scattering of E_i; σ_{D_i}, scattering of D_i; σ_{t_i}, scattering of t_i.

These values of the standard deviation must change if the data set is changed. However, it is assumed that the data set analyzed in this study is a standard one.

7.2 Example of synthetic accelerogram

Although we may be able to synthesize quasi-realistic accelerograms for future earthquakes, we should now examine the reliability of the synthetic accelerogram. For this purpose, sample accelerograms are synthesized by using the source, the path, and the site parameters of the Miyagi-Oki earthquake of June 12, 1978.

The source process of the Miyagi-Oki earthquake was studied by SENO *et al.* (1980) and HIRASAWA (1980), and the source parameters, L=56 km, r=73 km (at Ofunato), r=70 km (at Shiogama), $E\{\tau\}$=70 bar, and $\sqrt{E\{\tau^2\}}$=112 bar were estimated. The layer parameters at Ofunato and Shiogama were given by KOBAYASHI *et al.* (1978) and HIRASAWA (1980) as shown in Table 3. The ground response is calculated by HASKELL's (1960) method and is smoothed to obtain $|G^*(f_i)|$. e^{-kf} in (23) is assumed to be comparable to the attenuation received by a wave to go and return back in the surface layers. Using the quality factor in Table 3, k is estimated to be 0.0 at Ofunato and 0.25 at Shiogama.

Using these parameters, five sample accelerograms at each site are synthesized and compared to the observed accelerograms, which were digitized by

KURATA *et al.* (1979). In this process, since E_i is defined as the sum of total power of the two horizontal component accelerograms, $E_i/2$ is used for the input data of the simulation method in order to obtain an average single horizontal component accelerogram. The constants of the media are assumed as follows; v_P=6.5 km/sec, v_S=3.5 km/sec, ρ=3.0 g/cm^3, and Q=400 at the source region, v_S=3.0 km/sec and ρ=2.5 g/cm^3 at the basement rock.

Table 3. Layer parameters.*

Station	Thickness (m)	Density (g/cm^3)	S-wave velocity (km/sec)	Quality factor
Ofunato	360	2.3	1.5	100
	—	2.5	3.0	—
Shiogama	24	1.6	0.08	8
	3	1.8	0.3	10
	93	2.0	0.7	30
	80	2.3	1.5	100
	—	2.5	3.0	—

* KOBAYASHI *et al.* (1978) and HIRASAWA (1980).

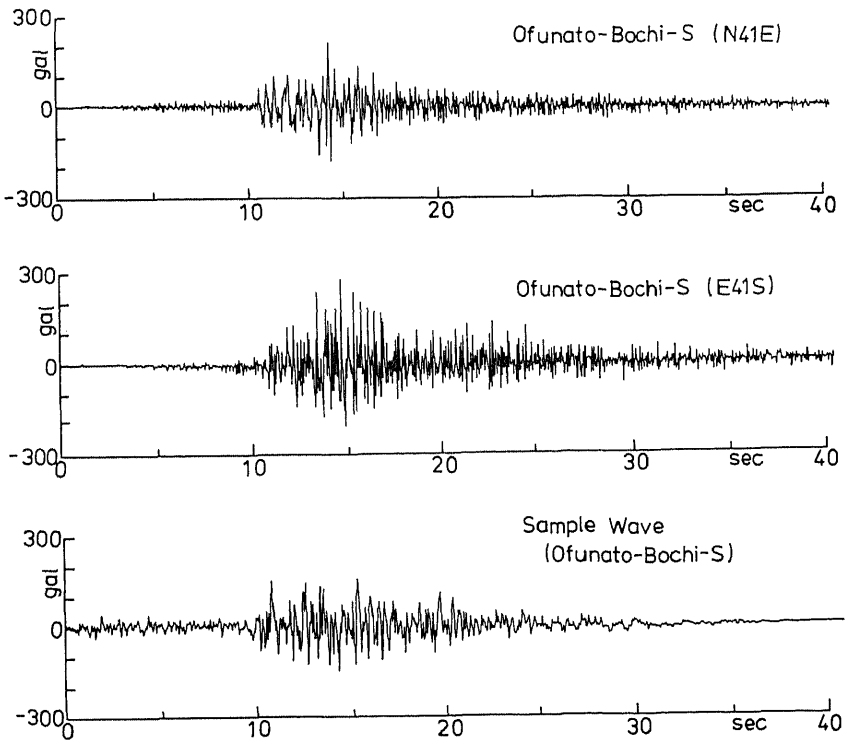

Fig. 11. Observed accelerograms and an example of synthetic accelerograms at Ofunato.

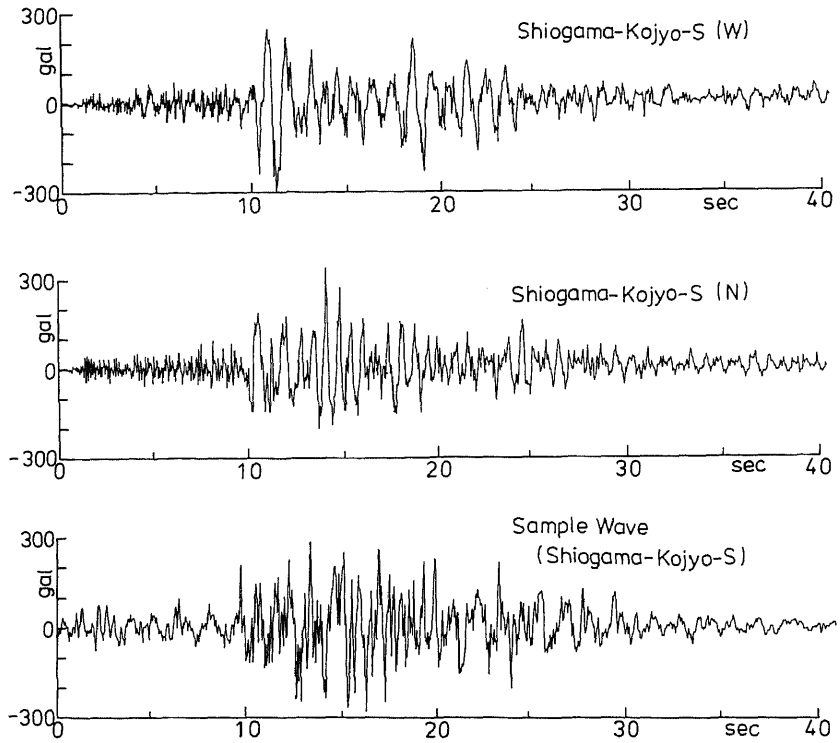

Fig. 12. Observed accelerograms and an example of synthetic accelerograms at Shiogama.

The wave-form and the running spectrum of one of the sample accelerograms are shown in Figs. 11–14 with those observed. In Table 4, the maximum acceleration, the total power, and the duration of the accelerograms are shown. Although the maximum acceleration of the sample accelerograms at Ofunato is somewhat too small and the total power of the sample accelerograms at Shiogama is somewhat too large, these samples seem to express the characteristics of the observed accelerograms well.

Synthetic accelerograms are needed to examine the resistance of complex buildings against earthquakes, or to carry out the elastic-plastic response analysis of structures. However, before the complex analyses, it must be examined whether the sample accelerograms can present the similar response spectra of one degree of freedom oscillator as those of observed accelerograms. In Figs. 15 and 16, the velocity response spectra of observed accelerograms are shown by the solid lines and the "mean$\pm$S.D." of the spectra of the five sample accelerograms are shown by the broken lines. Although there are some discontents, the response spectra of the sample accelerograms explain the differences in shape and amplitude between the spectra observed at each site.

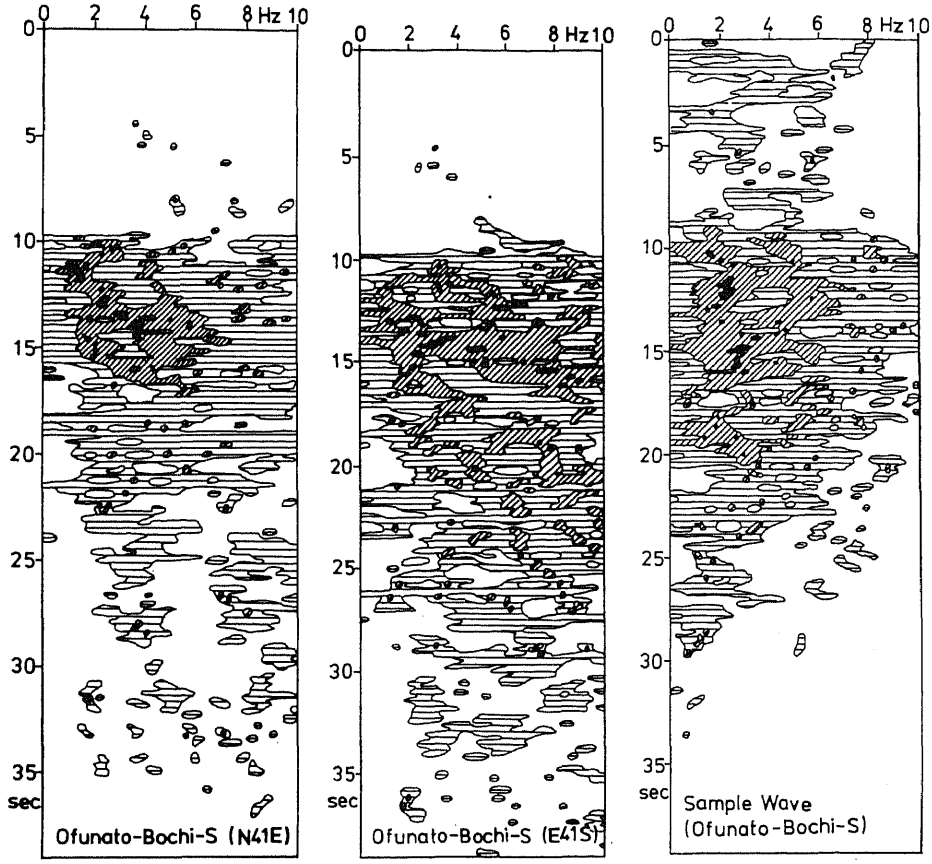

Fig. 13. Running power spectra of observed and an example of synthetic accelerograms at Ofunato. The dark region denotes that the amplitude is more than 10^8 gal^2·sec. Hatched regions are following it every 1/10 in amplitude.

8. *Conclusion*

Characteristics of ground acceleration due to earthquakes are expressed by the model parameters: E_i, the total power of the acceleration filtered by a narrow band-pass filter; D_i, the duration of filtered acceleration; and t_i, the starting time of the strong motion of filtered acceleration.

A model for synthesizing quasi-realistic strong ground motion is presented by analyzing the accelerograms of the Matsushiro earthquake swarm from 1965 to 1970 statistically. The probabilistic source model of HIRASAWA (1980) is used to estimate the amplitude of acceleration radiated from an earthquake source, so the present model is not strongly restricted by the limitation of the data set which was analyzed.

The duration of strong ground motion is found to have a relation to the

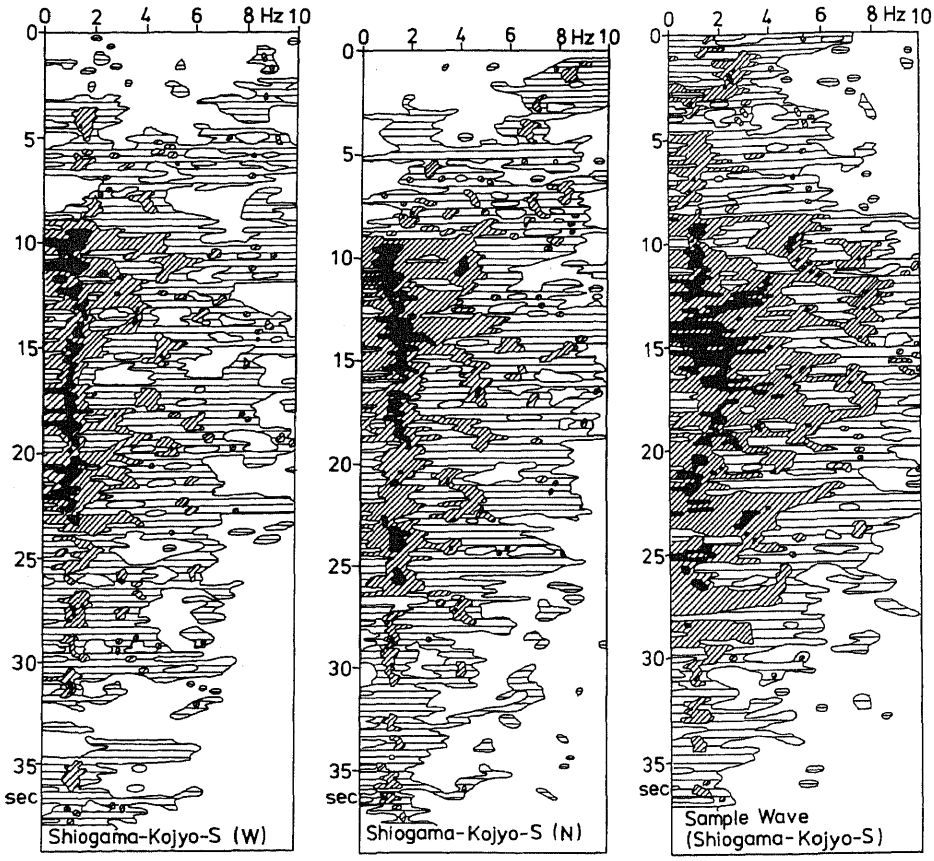

Fig. 14. Running power spectra of observed and an example of synthetic accelerograms at Shiogama. The amplitude is expressed by the same way as in Fig. 13.

Table 4. Maximum acceleration, total power, and duration of observed and sample accelerograms.

Ofunato-Bochi-S	Observed wave		Sample wave			
	N41E	E41S	Minimum	Maximum	Average	Standard deviation
Maximum acceleration (gal)	212.4	283.3	137.5	214.3	160.6	27.7
Total power ($\times 10^4$ gal^2·sec)	2.64	5.26	2.79	3.69	3.25	0.35
Duration (sec)	9.1	10.6	9.4	13.6	11.1	1.0
Shiogama-Kojyo-S	Observed wave		Sample wave			
	W	N	Minimum	Maximum	Average	Standard deviation
Maximum acceleration (gal)	296.0	336.8	285.3	432.5	345.8	54.6
Total power ($\times 10^5$ gal^2·sec)	1.29	1.15	1.78	2.46	2.18	0.22
Duration (sec)	11.4	13.3	11.7	17.7	14.9	2.5

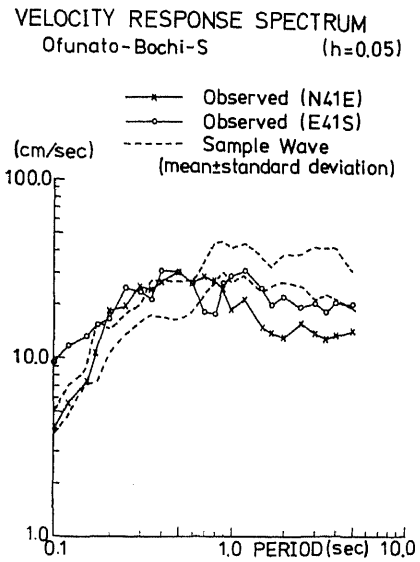

Fig. 15

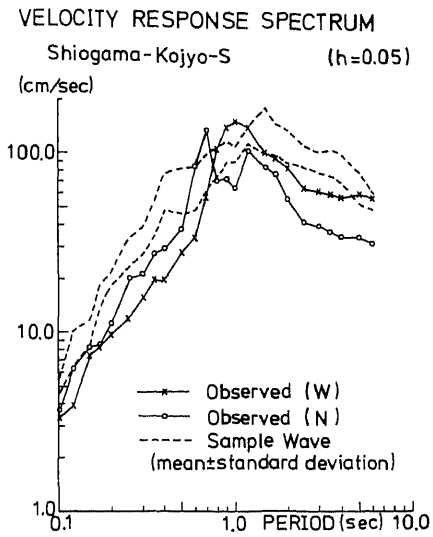

Fig. 16

Fig. 15. Velocity response spectra of observed and synthetic accelerograms at Ofunato. h indicates the damping coefficient of the oscillator. Solid lines denote the spectra of observed accelerograms and broken lines denote the "mean±S.D." of response spectra of five synthetic accelerograms.

Fig. 16. Velocity response spectra of observed and synthetic accelerograms at Shiogama. The notations are the same as those in Fig. 15.

amplification characteristic of surface layers at the sites. Assuming a simple relation between them, the influence of site condition on the duration is considered in estimating the model parameter, D_i.

Sample accelerograms synthesized by using the source parameters of the Miyagi-Oki earthquake of June 12, 1978 (M=7.4) seems to express the characteristics of the recorded accelerograms well. Therefore, this statistical model can be used for predicting quasi-realistic strong ground motions of future earthquakes although various assumptions are necessarily made to develop it.

The author wishes to express his hearty thanks to Mr. Hideo Motooka of the Kyowa Consultants for his valuable discussions during the course of this study. The author indebted to Miss Uki Koizumi of the Shinshu University for her help in preparing the data cards. Prof. Hiroo Kanamori and Dr. Robert Geller critically read the manuscript and provided many valuable comments. A computer HITAC M-200H of the Computer Center, the University of Tokyo, was used through the Remote Station of the Shinshu University.

Appendix. Simulation Method

A shot noise process filtered by a band-pass filter, $h_i(t)$, is

$$\bar{z}_i(t)=\sum_{k=1}^{N} Y_k h_i(t-\tau_k)\,, \tag{A1}$$

where N is the total number of pulses, Y_k are the pulse amplitudes and τ_k are the pulse arrival times. When Y_k are given as the probability variables with $\mathrm{E}\{Y_k\}=0$ and $\mathrm{E}\{Y_k^2\}=1$, the power spectral density of $\bar{z}_i(t)$ is

$$S_{\bar{z}_i}(f)=\lambda_0|H_i(f)|^2\,, \tag{A2}$$

where λ_0 is the arrival rate of pulses, and

$$H_i(f)=\int_{-\infty}^{\infty} h_i(t)\mathrm{e}^{-i2\pi ft}\mathrm{d}t\,. \tag{A3}$$

The expected value of $[\bar{z}_i(t)]^2$ is

$$\mathrm{E}\{[\bar{z}_i(t)]^2\}=\lambda_0\int_{-\infty}^{\infty}|H_i(f)|^2\mathrm{d}f\,. \tag{A4}$$

Now, a ground acceleration, $x(t)$, is nonstationary, so a filtered acceleration,

$$y_i(t)=x(t)*h_i(t)\,, \tag{A5}$$

is also nonstationary. The mean-square value of $y_i(t)$ during the time from t to $t+\Delta t$ is approximated as

$$\overline{[y_i(t)]_2}=\frac{1}{\Delta t}\int_t^{t+\Delta t}[y_i(t)]^2\mathrm{d}t\approx E_i\frac{\mathrm{d}C_i(t)}{\mathrm{d}t}\,, \tag{A6}$$

where E_i is the total power of $y_i(t)$, and $C_i(t)$ is the approximation function of the cumulative power curve as defined in Sec. 3. If the power spectral density of $x(t)$ is assumed to be smooth enough comparing with the width of the band-pass filter, $y_i(t)$ may be roughly simulated by $\bar{y}_i(t)$, which is a filtered shot-noise process multiplied by a shape function,

$$\bar{y}_i(t)=\left\{\sum_{k=1}^{N} Y_k h_i(t-\tau_k)\right\}\phi_i(t)\,. \tag{A7}$$

Comparing (A4) with (A6), the shape function is supposed as

$$\phi_i(t)=\left[\frac{E_i}{\lambda_0\displaystyle\int_{-\infty}^{\infty}|H_i(f)|^2\mathrm{d}f}\,\frac{\mathrm{d}C_i(t)}{\mathrm{d}t}\right]^{1/2}. \tag{A8}$$

Then, all of $\bar{y}_i(t)$, which simulate each of the filtered accelerograms individually, are superimposed to give a single simulated accelerogram of $x(t)$.

REFERENCES

AKI, K., Scaling law of earthquake source time-function, *Geophys. J. R. Astron. Soc.*, **31**, 3–25, 1972.

BOLT, B. A., Duration of strong ground motion, 5th World Conf. Earthquake Eng., Rome, 6-D, Paper No. 292, 1973.

DOBRY, R., I. M. IDRISS, and E. NG, Duration characteristics of horizontal components of strong-motion earthquake records, *Bull. Seismol. Soc. Am.*, **68**, 1487–1520, 1978.

GOTO, H., H. KAMEDA, and M. SUGITO, Prediction of strong earthquake motions by evolutionary process model, *Proc. Japan Soc. Civil Eng.*, No. 286, 37–51, 1979 (in Japanese).

FURUYA, I., Predominant period and magnitude, *J. Phys. Earth*, **17**, 119–126, 1969.

HASKELL, N. A., Crustal reflection of plane SH waves, *J. Geophys. Res.*, **65**, 4147–4150, 1960.

HASKELL, N. A., Total energy and energy spectral density of elastic wave radiation from propagating faults, *Bull. Seismol. Soc. Am.*, **54**, 1811–1841, 1964.

HIRASAWA, T., Seismic activity, General Report on the 1978 Miyagiken-Oki Earthquake, Tohoku Branch of Japan Soc. Civil Eng., Chap. 2, Apr. 1980 (in Japanese).

KANAI, K., T. TANAKA, T. MORISHITA, and K. OSADA, Observation of microtremors. XI. Matsushiro earthquake swarm area, *Bull. Earthq. Res. Inst. Univ. Tokyo*, **44**, 1297–1333, 1966.

KATADA, T. and M. HOSHIYA, Statistical prediction of earthquake acceleration wave, *Proc. Japan Soc. Civil Eng.*, No. 298, 9–15, 1980 (in Japanese).

KOBAYASHI, H., K. SENO, and S. MIDORIKAWA, Strong ground motions and seismic microzoning. Part I, A Report on the Miyagi-Oki Earthquake of June 12, 1978, 2nd Int. Conf. Microzonation, Nov. 1978, 1–13, 1978.

KURATA, E., S. IAI, Y. YOKOYAMA, and H. TSUCHIDA, Strong-motion earthquake records on the 1978 Miyagi-Ken-Oki earthquake in port areas, *Tech. Note Port Haber Res. Inst.*, No. 319, June 1979 (in Japanese).

MCCANN, M. W., Jr. and H. C. SHAH, Determining strong-motion duration of earthquakes, *Bull. Seismol. Soc. Am.*, **69**, 1253–1265, 1979.

OSAWA, Y., T. TANAKA, M. SAKAGAMI, and S. YOSHIZAWA, Digital Data of the Strong-Motion Earthquake Accelerograms in Matsushiro earthquake Swarm Area, Earthquake Research Institute the University of Tokyo, Apr. 1976 (in Japanese).

OTSUKA, M., Earthquake magnitude and surface fault formation, *J. Phys. Earth*, **12**, 19–24, 1964.

OTSUKA, M., A new parameter for prediction of earthquake disaster, Proc. Meet. Seismol. Soc. Japan, C-35, May 1979 (in Japanese).

SEED, H. B., R. V. WHITMAN, H. DEZFULIAN, R. DOBRY, and I. M. IDRISS, Soil conditions and building damage in 1967 Caracas earthquake, *J. Soil Mech. Div., Proc. Am. Soc. Civil Eng.*, **98**, 787–806, 1972.

SENO, T., K. SHIMAZAKI, P. SOMERVILLE, K. SUDO, and T. EGUCHI, Rupture process of the Miyagi-Oki, Japan, earthquake of June 12, 1978, *Phys. Earth Planet. Inter.*, **23**, 39–61, 1980.

TRIFUNAC, M. D. and A. G. BRADY, A study on the duration of strong earthquake ground motion, *Bull. Seismol. Soc. Am.*, **65**, 581–626, 1975.